Loss of glial fibrillary acidic protein (GFAP) impairs Schwann cell proliferation and delays nerve regeneration after damage

Daniela Triolo[1], Giorgia Dina[1], Isabella Lorenzetti[1], MariaChiara Malaguti[1,2], Paolo Morana[3], Ubaldo Del Carro[2,3], Giancarlo Comi[2,4], Albee Messing[5], Angelo Quattrini[1,2] and Stefano C. Previtali[1,2,*]

[1]Neuropathology Unit, [2]Department of Neurology and INSPE, and [3]Neurophysiology Unit, San Raffaele Scientific Institute, Via Olgettina 60, 20132 Milan, Italy
[4]Università Vita-Salute San Raffaele, 20132 Milan, Italy
[5]Waisman Center and Department of Comparative Biosciences, University of Wisconsin-Madison, Madison, WI 53706, USA
*Author for correspondence (e-mail: previtali.stefano@hsr.it)

Accepted 14 July 2006
Journal of Cell Science 119, 3981-3993 Published by The Company of Biologists 2006
doi:10.1242/jcs.03168

Summary

Axonal loss causes disabling and permanent deficits in many peripheral neuropathies, and may result from inefficient nerve regeneration due to a defective relationship between Schwann cells, axons and the extracellular matrix. These interactions are mediated by surface receptors and transduced by cytoskeletal molecules. We investigated whether peripheral nerve regeneration is perturbed in mice that lack glial fibrillary acidic protein (GFAP), a Schwann-cell-specific cytoskeleton constituent upregulated after damage. Peripheral nerves develop and function normally in GFAP-null mice. However, axonal regeneration after damage was delayed. Mutant Schwann cells maintained the ability to dedifferentiate but showed defective proliferation, a key event for successful nerve regeneration. We also showed that GFAP and the other Schwann-cell-intermediate filament vimentin physically interact in two distinct signaling pathways involved in proliferation and nerve regeneration. GFAP binds integrin αvβ8, which initiates mitotic signals soon after damage by interacting with fibrin. Consistently, ERK phosphorylation was reduced in crushed GFAP-null nerves. Vimentin instead binds integrin α5β1, which regulates proliferation and differentiation later in regeneration, and may compensate for the absence of GFAP in mutant mice. GFAP might contribute to form macro-complexes to initiate mitogenic and differentiating signaling for efficient nerve regeneration.

Key words: Cytoskeleton, Transgenic mice, Extracellular matrix, Nerve regeneration, Adhesion

Introduction

Axonal loss and defective axonal regeneration is responsible for severe and permanent deficits in peripheral neuropathy. Although axonal loss might not affect the life span of a patient, it results in severe disability with progressive muscle atrophy and weakness, sensory deficits, and foot and leg abnormalities. Any improvement in regeneration would benefit these patients.

Efficient axonal regeneration relies on the pathogenetic mechanism that caused the axonal degeneration. If the disease primarily affects the neuronal cell body (sensory or motor neurons), the damage mostly prevents recovery. Conversely, when the neuronal cell body is preserved, the regeneration capacity should be maintained but still depends on the permissive environment in the nerve. In the latter case, the nerve regeneration results from balanced interaction of Schwann cells, the environment – the extracellular matrix (ECM) – and regrowing axons (Scherer and Salzer, 2001; Stoll and Muller, 1999).

All the events involved in axonal regeneration can be recapitulated in the model of Wallerian degeneration-regeneration, which is induced in rodents by traumatic crush injury of the sciatic nerve. The spatial-temporal events associated with degeneration and regeneration have been extensively documented and consist of a series of stereotyped steps (Griffin and Hoffman, 1993; Scherer and Salzer, 2001). The segments of axons distal to the site of injury degenerate, and macrophages penetrate and remove the disrupted myelin sheets, while Schwann cells dedifferentiate, re-enter the cell-proliferation cycle and provide a substrate for axonal regrowth. The onset of mitogenesis is synchronous with a peak 3-5 days after injury and requires a prelude phase of intense rearrangement of the Schwann-cell cytoplasm. During this process Schwann cells acquire again the expression of surface molecules characteristic of embryonic development, such as neural cell adhesion molecule (NCAM), L1-adhesion molecule and $p75^{NTR}$, and upregulate cytoskeletal constituents, such as glial fibrillary acidic protein (GFAP) and vimentin (Jessen et al., 1990; Martini, 1994; Neuberger and Cornbrooks, 1989). After proliferation, Schwann cells interact with molecules in the extracellular environment to reorganize the basement membrane and to rearrange themselves into bands of Bungner. These bands are rail-track-like structures upon which axons can efficiently regenerate. Further steps in nerve regeneration include Schwann cells that surround bundles of regenerating axons, segregate larger axons into 1:1 relationship, enwrap them and form myelin sheaths.

Most of these latter events reproduce what occurs in development (Webster, 1993), and rely on the interaction of Schwann cell surface receptors with molecules that normally form the ECM endoneurium or infiltrate the nerve because of the blood-nerve barrier disruption (Akassoglou et al., 2002; Feltri et al., 2002; Lefcort et al., 1992; Patton et al., 1997; Previtali et al., 2003b). These complex interactions result in a continuous reorganization of the Schwann cell cytoskeleton that operates either downstream the outside-in or upstream the inside-out signaling pathway (Previtali et al., 2001).

GFAP is a glial-specific member of the intermediate filament family, which includes cell-type-specific filamentous proteins with similar structure and function as scaffold for cytoskeleton assembly and maintenance (Coulombe and Wong, 2004). During development, Schwann cells express two other intermediate filaments: nestin and vimentin (Dong et al., 1999; Jessen and Mirsky, 1991). GFAP appears at a relatively late stage in Schwann cell development, essentially when immature Schwann cells are formed, and is downregulated in those Schwann cells that form myelin (Jessen et al., 1990). After birth, only non-myelin-forming Schwann cells and Schwann cells that dedifferentiate after nerve injury express GFAP, whereas myelin-forming Schwann cells express vimentin (Jessen et al., 1990; Mirsky and Jessen, 2005).

GFAP is also expressed in astrocytes, a Schwann cell counterpart in the central nervous system (CNS). The upregulation of GFAP, together with vimentin, was thought to be a crucial step for astrocyte activation in response to brain damage. However, deletion of GFAP in mutant mice did not result in any gross CNS abnormality (Gomi et al., 1995; Liedtke et al., 1996; McCall et al., 1996; Pekny et al., 1995) or in defective response to CNS injury (Pekny et al., 1999). Impaired astrocyte reaction to injury was only observed in double GFAP-vimentin-deficient mice (Pekny et al., 1999).

By contrast, there are no extensive reports on the effects of GFAP deletion on peripheral nerve development and function, or on the possible consequences for nerve regeneration. Here, we examined the peripheral nervous system of GFAP-null mice. We observed normal nerve development and adult nerve function. No morphological abnormalities were detected despite different composition of the Schwann cell cytoskeleton and endoneurial ECM. However, the lack of GFAP delayed nerve regeneration after damage, probably due to defective Schwann cell proliferation. We also found that GFAP and vimentin associate with two different adhesion pathways. GFAP complexes with integrin αvβ8, which binds fibrin and modulates Schwann cell proliferation after damage. Consistently, we found reduced phosphorylation of ERK1/2 in injured sciatic nerves of GFAP-null mice. Vimentin, instead, associates with integrin α5β1 and fibronectin, and regulates the subsequent steps of Schwann cell proliferation and nerve regeneration.

Results

Loss of GFAP does not impair peripheral nerve development and function

The effects of GFAP deletion have been previously analyzed in the CNS (reviewed in Messing and Brenner, 2003; Privat, 2003), whereas consequences on the peripheral nervous system have not been investigated in detail. To this aim, we analyzed peripheral nerve development and function in GFAP null mice.

First we confirmed that homozygous mutant mice did not synthesize GFAP in Schwann cells. We performed immunohistochemistry and western blot analysis of the sciatic nerve. Both experiments showed absence of the GFAP protein (Fig. 1A,B, and data not shown).

Then, we investigated whether peripheral nerve development was impaired. We compared semi-thin and ultra-thin sections from the sciatic nerve of postnatal day (P) P1, P7, P14, P28 and P60 GFAP-null mice to age-matched controls. No significant differences in axonal sorting, Schwann-cell axon relationship and myelination were observed (Fig. 1C-J). Myelin-forming and non-myelin-forming Schwann cells did not show cyto-architectural abnormalities; in particular, we did not observe filament aggregates or any other abnormalities in the basement membrane (Fig. 1K).

We then determined the absolute number of myelinated fibers and performed morphometric analysis comparing the sciatic nerve of GFAP-null mice those of wild type. The total number of myelinated fibers, fiber diameter and myelination (g-ratio) was not significantly different in GFAP-null mice and wild-type littermates (Fig. 1L,M).

To confirm morphological data we performed functional tests. Mutant mice appeared normal from birth to 15 months of age. They walk, run, climb and reproduce similarly to age-matched controls. At 3 and 6 months, the GFAP null mice and wild-type littermates showed no significant difference in rotarod testing (Fig. 1M). Consistent with behavioral analysis, GFAP-null mice showed normal nerve conduction velocity (NCV) (35±0.5 m/second) and compound motor action potentials (cMAP) (37±0.7 mV) in the neurophysiological tests (Fig. 1N).

The absence of GFAP is probably compensated by other intermediate filaments and modifies the endoneurial ECM composition

We investigated whether other intermediate filaments can compensate for the absence of GFAP in mutant mice, thus explaining the normal phenotype. In fact, during development, two other intermediate filaments are described in Schwann cells: nestin and vimentin (Dong et al., 1999; Jessen and Mirsky, 1991).

First, we performed qualitative analysis by immunohistochemistry. Results showed similar expression of vimentin in non-myelin-forming Schwann cells, as depicted by colocalization with L1, in GFAP-null mice and controls (compare Fig. 2A-C with 2G-I). Accordingly, vimentin was similarly expressed in myelin-forming Schwann cells, identified by myelin-associated glycoprotein (MAG), in both mutants and controls (compare Fig. 2D-F with 2J-L). Nestin was similarly expressed in myelin-forming and non-myelin forming Schwann cells in both GFAP-null and wild-type controls (data not shown). To test whether the absence of GFAP alters expression of the other intermediate filaments quantitatively, we performed western blot analysis. Western blots of total nerve lysate did not show significant differences in the amount of vimentin and nestin in nerves of GFAP-null mice compared with controls (Fig. 2M).

Manipulation of the cytoskeleton might alter outside-in and inside-out signaling as shown in the CNS of GFAP-vimentin double mutants (Menet et al., 2001). We therefore investigated the expression of surface receptors and ECM molecules

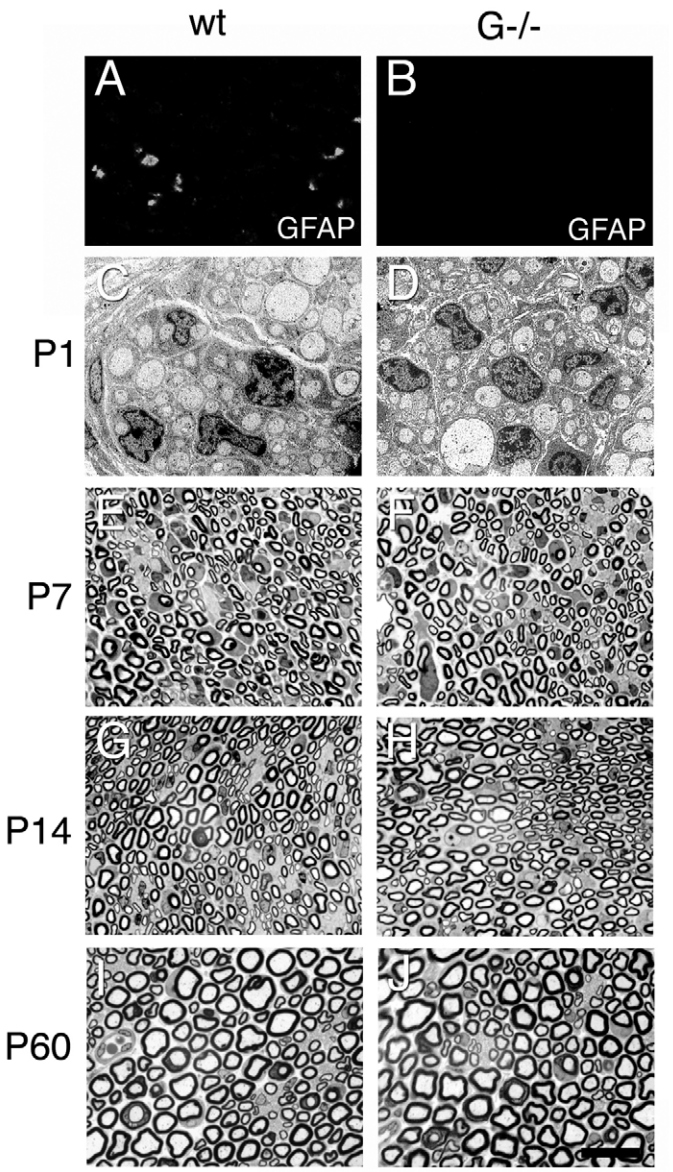

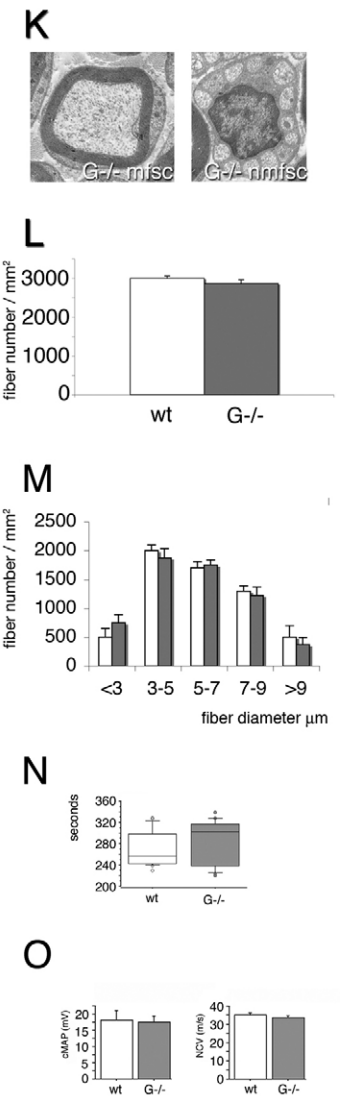

Fig. 1. Morphological and functional analysis of the sciatic nerve in GFAP-null mice. (A,B) Staining for GFAP in nerves of wild-type and GFAP-null sciatic mice; GFAP is absent in nerves of the mutant. Ultra-thin (C,D) and semi-thin (E-J) section analysis of sciatic nerves from control and GFAP-null mice at 1, 7, 14 and 60 days after birth. No significant differences were observed. (K) Ultra-thin sections of the sciatic nerve from 2-months old GFAP-null mice. Both myelin-forming and non-myelin forming Schwann cells showed normal features. (L) Myelin-fiber density in adult sciatic nerve from control and GFAP-null mice. No significant differences were observed. (M) Morphometry of myelinated axons in adult sciatic nerve from control and mutant mice. No significant differences were observed per number and size distribution. (N) Rotarod test analysis and (O) electrophysiological analysis performed in mutant and control mice of 2 months of age. No significant differences were observed. Bar in J, 30 μm for A,B; 8 μm for C,D; 20 μm for E-J; 5 μm for K.

previously described in the peripheral nerve (Previtali et al., 2001; Previtali et al., 2003b). By immunohistochemistry, we did not observe differences in the expression of integrins (α1, α2, α3, α6, α7, β1, β4), β-dystroglycan, L1 and NCAM in Schwann cells of GFAP-null mice, or of collagen IV and laminin chains α2, α4, β1 and γ1 in the endoneurium. Similarly, we did not observe differences in the expression of collagen IV, fibronectin, vitronectin and laminin chains α1, α5, β2, γ1 and γ3 in the perineurium and blood vessels. Only fibronectin showed higher expression in the endoneurium of GFAP-null mice compared with controls (compare Fig. 2N,O with 2P,Q, and data not shown). Western blot confirmed the increased amount of fibronectin, whereas other ECM components, such as collagen IV or laminins were expressed at similar levels (Fig. 2R).

Regeneration of sciatic nerve after injury is impaired in GFAP-null mice

Since efficient nerve regeneration requires Schwann cells contribution and is associated with upregulation of intermediate filaments in Schwann cells, we examined nerve regeneration in GFAP-null mice. Sciatic nerves from GFAP-null mice and age-matched controls were crushed and examined 3 mm and 10 mm distal to the site of injury 3, 7, 10, 15, 21 and 45 days after injury. Results showed a clear delay in nerve regeneration and remyelination in GFAP-null mice. Data for both distances were concordant.

Three days after injury both wild-type and GFAP-null mice showed diffuse signs of degeneration, including myelinolysis, myelin debris and axonal fragmentation (data not shown). Seven and ten days after injury, in wild-type nerves, we observed some features of axonal degeneration, some macrophages and some bands of Bungner. However, the prominent aspect was the presence of many regrowing axons, some organized in clusters of regeneration, some arranged in a 1:1 ratio with Schwann cells, and few ensheathed with thin myelin, indicating remyelination (Fig. 3A,A^{I}). By contrast, in nerves of GFAP-null mice we observed diffuse signs of

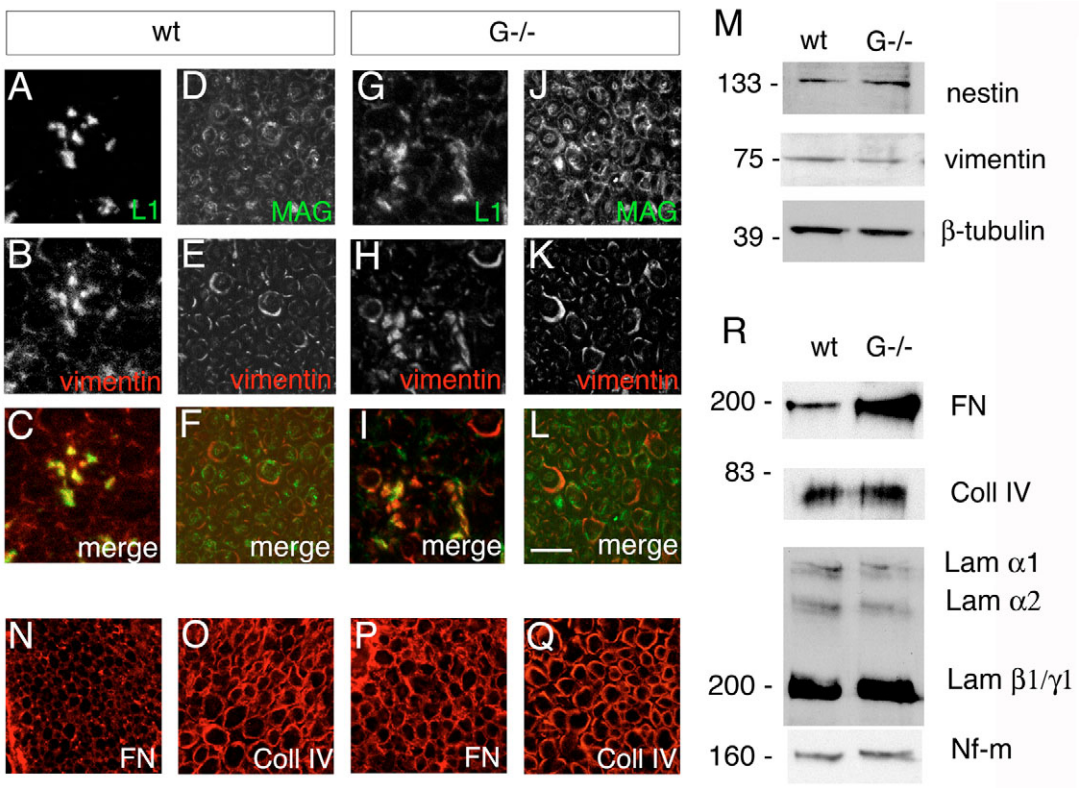

Fig. 2. Expression of intermediate filaments and ECM constituents in the sciatic nerve of GFAP-null mice. (A-C) Double staining for L1 and vimentin (merge in C) shows vimentin expression in non-myelin-forming Schwann cells. (D-F) Double-staining for MAG and vimentin (merge in F) shows vimentin expression in myelin forming Schwann cells. (G) Western blot analysis shows comparable levels of nestin and vimentin in mutants compared with wild type; β-tubulin was used to normalize the samples. (H,I) Fibronectin expression in sciatic nerves of wild-type and GFAP-null mice; an increased amount of fibronectin was observed in the endoneurium in mutants. (J,K) Collagen IV expression in sciatic nerves of wild-type and GFAP-null mice. Mutants and controls showed comparable levels of collagen IV. (L) Western blot analysis confirmed an increased amount of fibronectin in the sciatic nerve of GFAP-null mice compared with controls, whereas collagen IV and laminins were present at equal amounts. SDS-PAGE gels were 7.5% except when analyzing laminins (5%). Bar in L, 60 μm for A-C; 20 μm for D-F and H-K.

ongoing axonal degeneration, invading macrophages and several Schwann cells arranged into Bungner bands (Fig. 3B,B^{I},B^{II}). Few clusters of regeneration and fibers in a 1:1 ratio and, rarely, thinly myelinated fibers were observed (Fig. 3B^{I},B^{II}). To quantify differences, we performed morphometric analysis counting all the fibers with a diameter >1 μm (fibers that were expected to undergo myelination). The average number of axons in nerves of GFAP-null mice was significantly reduced compared with those of wild type, by 33% at 3 mm and 53% at 10 mm to the site of injury (P<0.05 and P<0.01 respectively; Fig. 3G,H). Interestingly, we found a higher percentage of myelinated vs non-myelinated fibers (59% vs 41%) in controls, whereas this relationship was the opposite in nerves of GFAP-null mice (25% myelinated vs 75% non-myelinated fibers). Moreover, fiber-diameter distribution confirmed a reduced number of fibers in nerves of GFAP-null mice at almost any diameter (Fig. 3I,J).

Fifteen and 21 days after injury, nerves of both wild-type and GFAP-null mice showed increased signs of regeneration (Fig. 3C,D, and data not shown). However, signs of degeneration and invading macrophages were preeminent in mutant nerves. The overall number of fibers was significantly reduced in nerves of GFAP-null mice compared with those of wild type. Twenty days after injury, mutant nerves showed 11-30% less fibers than controls (P=0.05 at 3 mm and P<0.01 at 10 mm; Fig. 3G,H). Fiber diameter distribution confirmed a reduced number of fibers at each diameter in nerves of GFAP-null mice, especially for those >3 μm (Fig. 3K,L).

Forty-five days after injury, a morphologically normal situation was essentially achieved in control nerves, whereas GFAP-null mice still showed signs of ongoing regeneration (Fig. 3E,F). Morphometric analysis confirmed that nerves of mutant mice contained roughly 20% less fibers than controls (P<0.05; Fig. 3G,H and 3M,N). We also detected thickening of the myelin sheath – represented as the g-ratio – which was significantly higher in nerves of GFAP-null mice compared with those of control animals (0.73±0.08 vs 0.69±0.09).

To confirm delayed nerve regeneration in nerves of GFAP-null mice, we performed two functional tests: motor-neuron retrograde labeling using fluorochrome-conjugated cholera toxin subunit B and neurophysiological analysis. A preliminary trial was performed in control mice to identify the first time point after sciatic crush injury at which fluorescent cholera toxin injected in gastrocnemius was detected in motor neurons. In control mice, motor neurons were labeled by fluorescent cholera toxin when injected 12 days after injury and sacrificed 48 hours later, at day 14. We therefore analyzed at this time point three GFAP-null mice and 3 age-matched controls. We

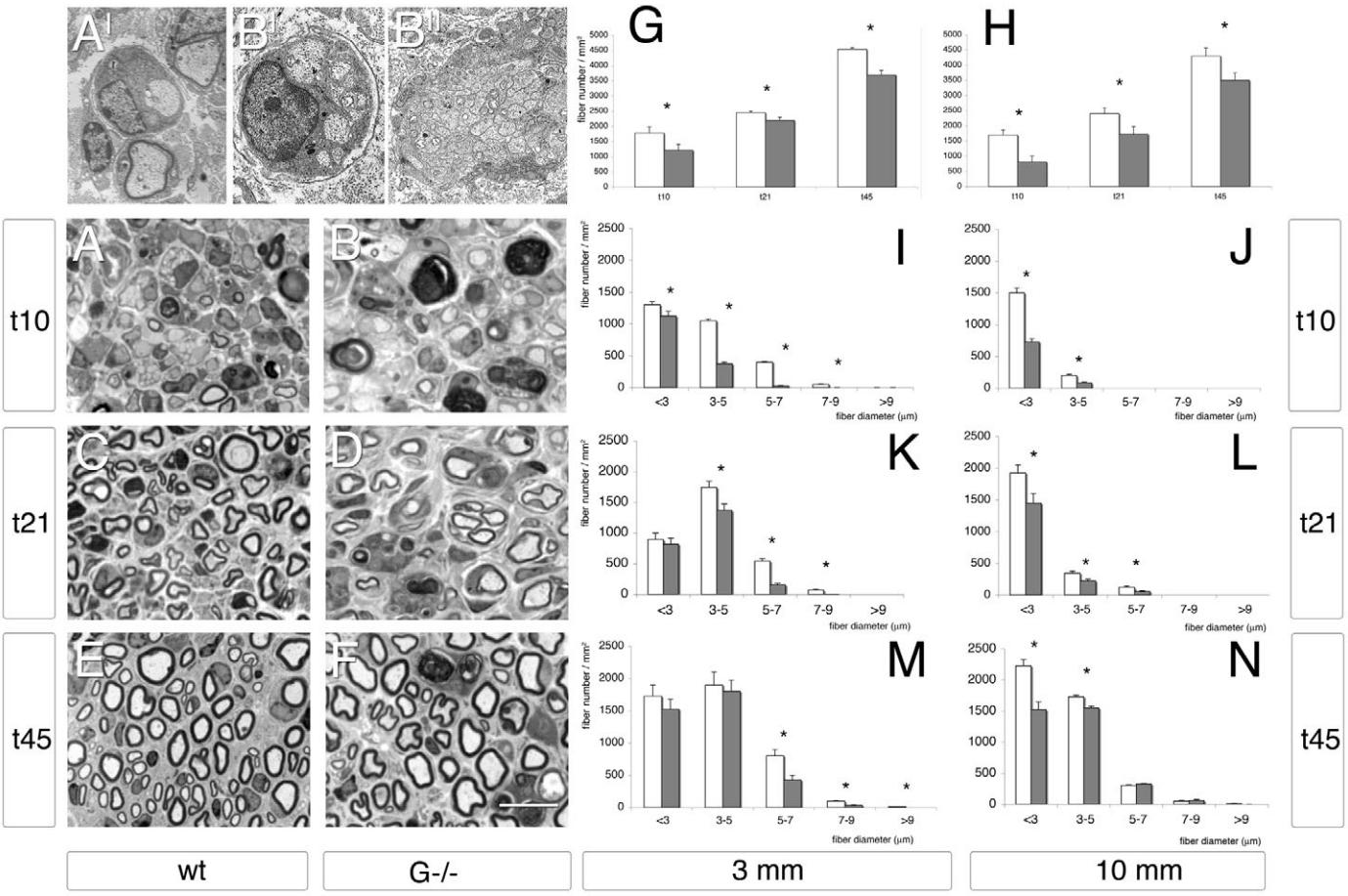

Fig. 3. Delayed nerve regeneration in the sciatic nerves of GFAP-null mice revealed by morphologic and morphometric analysis. (A-F) Light-microscopy images of injured nerves of GFAP-null mice, 3 mm distal to the lesion, compared with age-matched controls at different time points. Electron microscopy images of t10 (ten days after crushing) nerve samples are shown in (A^{I}) for control and (B^{I},B^{II}) for mutant mice. Ten days after crushing, nerves of control mice showed several fibers in 1:1 ratio as well as thinly myelinated fibers (A,A^{I}), whereas in nerves of mutant mice Schwann cells prevailed that were still sorting axons (B,B^{I}) and bands of Bungner (B^{II}). Twenty-one days after crushing, maturation of nerves in control mice was evident (C) whereas nerves of mutant mice still showed several degenerating fibers and clusters of regeneration (D). Forty-five days after crush, nerves of controls were nearly normal (E) whereas nerves of GFAP-null mice contained degenerating and thinly myelinated fibers (F). (G-N) Morphometric analysis of regenerating nerves at different time points, comparing data obtained 3 mm and 10 mm distally to the site of injury. (G,H) Diagram of the total number of fibers at 10, 21 and 45 days after injury; nerves of GFAP-null mice always showed significantly reduced number of fibers. (J-N) Diagram of the regenerating nerves at different time points subdivided per fiber diameter; results show reduced number of regenerating fibers in nerves of mutant mice, primarily those with larger diameter. Error bars represent the +s.e.m. Bar in F, 10 μm for A-F; 6 μm for A^{I}; 3 μm for B^{I},B^{II}. *P<0.05.

observed in GFAP-null mice that only 6% of motor neurons were labeled by the fluorescent dye, whereas in control mice it was 20% (P<0.001; Fig. 4A).

Consistent with the above results, GFAP-null mice showed neurophysiological signs of delayed regeneration (Fig. 4B). Ten days after crushing, we did not detect any signal in either GFAP-null or control mice, in agreement with motor neuron dye labeling, which showed target-muscle innervation only after day 12. Fifteen days after injury, amplitudes of distal cMAP in GFAP-null mice were 40% of those in control mice (0.8±0.4 vs 1.4±0.1 mV; P=0.02), whereas NCVs were similar (9.5±1 vs 10±2 m/second). At 21 days after crushing, amplitudes in GFAP-null mice were still 50% of those in controls (0.9±0.1 vs 1.9±0.3 mV; P=0.01) with similar NCVs (11.4±1 vs 12.5±2 m/second). Finally, 45 days after injury, GFAP-null mice showed amplitudes 40% of those in controls (5.6±2 vs 10.4±2 mV; P=not significant) and NCVs 20% slower (16±1 vs 20±1 m/second; P=not significant) although differences were not significant.

Loss of GFAP does not affect Schwann cell dedifferentiation and cytoskeleton rearrangement

To obtain efficient nerve regeneration after damage, Schwann cells have to dedifferentiate, proliferate, and provide a favorable environment for axonal regrowth. A defect in one of these Schwann cell functions that implies the continuous rearrangement of the cytoskeleton may explain the delay of regeneration in GFAP mutants.

First, we evaluated whether GFAP-null Schwann cells normally dedifferentiate and modulate the cytoskeleton in response to crush injury. After damage Schwann cell dedifferentiation results in the downregulation of myelin genes

and the re-expression of genes such as those encoding NCAM, L1-molecule and $p75^{NTR}$, along with the upregulation of GFAP and vimentin (Jessen et al., 1990; Martini, 1994; Neuberger and Cornbrooks, 1989). In GFAP-null mice, by 3 days after damage, we observed that mutant Schwann cells regularly dedifferentiated and expressed NCAM, L1 $p75^{NTR}$ and vimentin (compare Fig. 5A,C,E,G with 5B,D,F,H respectively). Then we evaluated whether vimentin was adequately upregulated in the sciatic nerve of GFAP null mice. We performed western blot analysis of the distal stump of the sciatic nerve and measured the amount of vimentin at 3, 6, 15, 21 and 45 days after injury in GFAP-null and control mice. Results showed that GFAP-null mice upregulate vimentin in injured nerves similarly to controls (Fig. 5I,J). Hence, defective regeneration was not the consequence of impaired Schwann cell dedifferentiation or insufficient vimentin upregulation.

Delayed nerve regeneration is probably due to reduced Schwann cell proliferation in GFAP-null mice

Since Schwann cell proliferation is a crucial step to initiate and obtain efficient nerve regeneration (Chen et al., 2005), and GFAP has been associated with cell mitosis (Yasui et al., 1998), we then focused our attention on Schwann cell proliferation. Previous reports showed that Schwann cells mainly proliferate in the first week after nerve damage, with a peak at day 3 (Clemence et al., 1989; Oaklander and Spencer, 1988; Pellegrino et al., 1986). Therefore, we performed crush injury of the sciatic nerve of six GFAP-null and six wild-type littermates. Three and 6 days after damage the animals were pulsed with BrdU to label cells in the DNA-synthesis phase of the cell cycle and then killed to perform BrdU staining. DAPI-

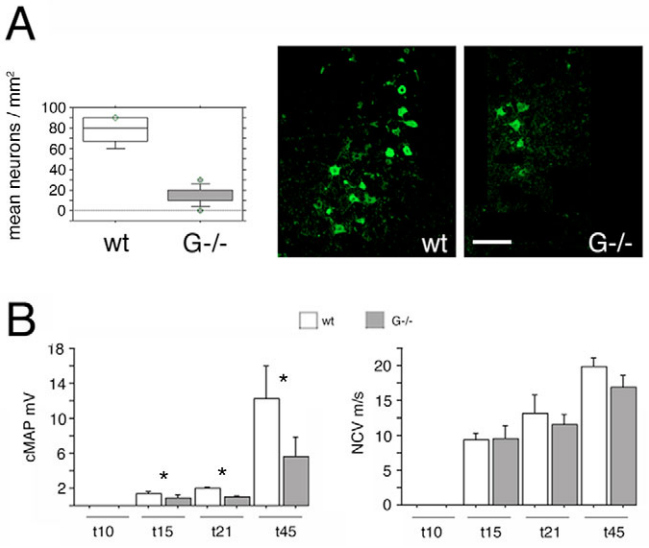

Fig. 4. Delayed nerve regeneration in nerves of GFAP-null mice measured by neurophysiology and motor neuron retrograde labeling with GFP-conjugated cholera toxin subunit B. (A) The total number of labeled motor neurons in the lumbar enlargement 48 hours after injection of fluorescent cholera toxin subunit B in the gastrocnemius is significantly reduced in GFAP-null mice compared with control mice. (B) Distal cMAP recordered in nerves of GFAP-null mice always showed amplitudes of half-values compared with controls, whereas NCVs did not show significant differences; *P<0.05. Bar, 50 μm.

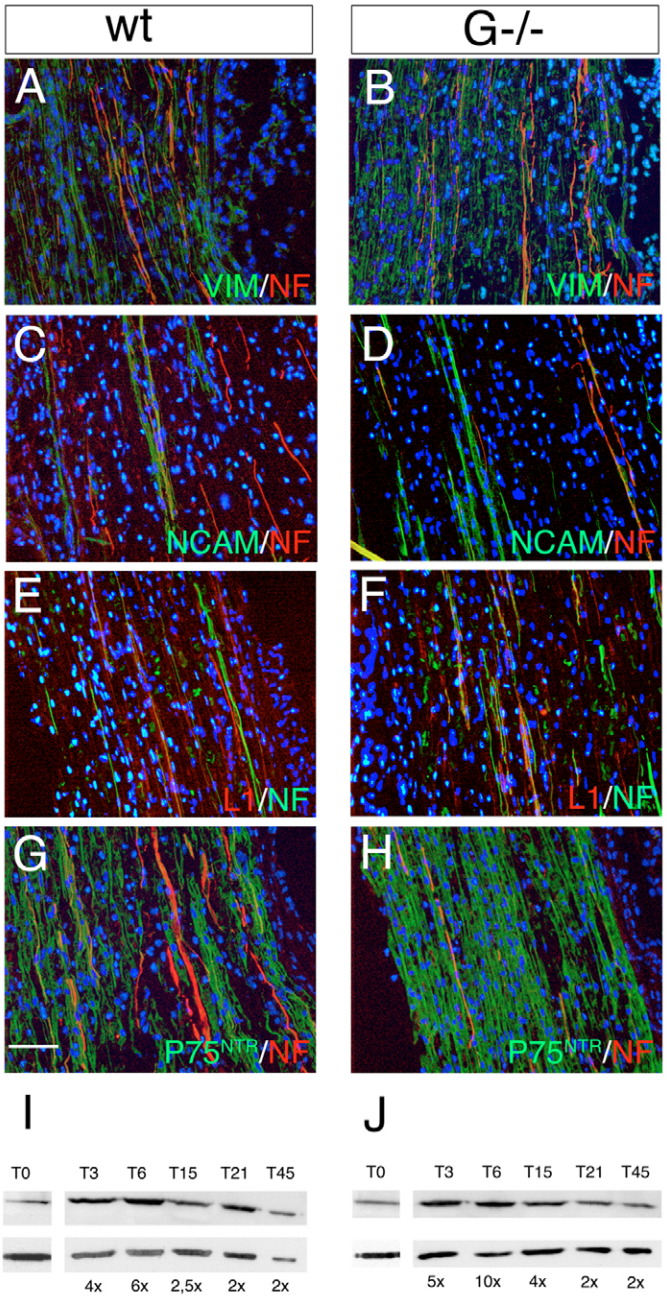

Fig. 5. Vimentin upregulation is maintained in nerves of GFAP-null mice after sciatic nerve injury. (A-H) Longitudinal sections of 3-day-old injured sciatic nerves from wild-type (A,C,E,G) and GFAP-null mice (B,D,F,H) double-stained for vimentin and neurofilaments (A,B), NCAM and neurofilaments (C,D), L1 and neurofilaments (E,F), p75NTR and neurofilaments (G,H). DAPI staining of nuclei (blue). The dedifferentiated Schwann cells showed expression of the above molecules as in wild type. Bar, 30 μm. (I,J) Protein extracts from the distal stump of crushed nerves from wild-type (I) and GFAP-null mice (J) at different time points were immunoblotted with an anti-vimentin antibody. Sample loading was normalized against β-tubulin. Ratio of vimentin to β-tubulin was measured by densitometry and expressed in the bottom line as times of increase at each time point T (in days) relative to T zero. Compared with control mice, vimentin is similarly upregulated in nerves of GFAP-null mice.

positive and S100-positive Schwann cell nuclei (DAPI$^+$ and S100$^+$) labeled with BrdU were counted in the distal stump of the sciatic nerve. Results showed a significant reduction in Schwann cell proliferation in GFAP-null mice at day 3 (8.3±0.5% vs 12.2±1.4%, P=0.04) and an almost significant reduction at day 6 (6.9±1.0% vs 9.7±1.0%, P=0.06) (Fig. 6A-E). To confirm these data, we performed similar double staining for phosphorylated histone H3 with an antibody that recognizes only proliferating cells in the mitotic phase of the cell cycle. Results confirmed a significant reduction of Schwann cell proliferation in the nerves of mutant mice both 3 days (5.5±1.2% vs 2.6±0.7%, P<0.001) and 6 days (3.5±0.8% vs 2.1±1.0%, P=0.04) after injury (Fig. 6F-J). However, we did not observe significant differences in Schwann cell apoptosis at days 3 and 6 (Fig. 6K-O).

GFAP and vimentin constitute different target molecules for integrin receptors involved in Schwann cell proliferation and nerve regeneration

Schwann cell proliferation and migration after nerve damage

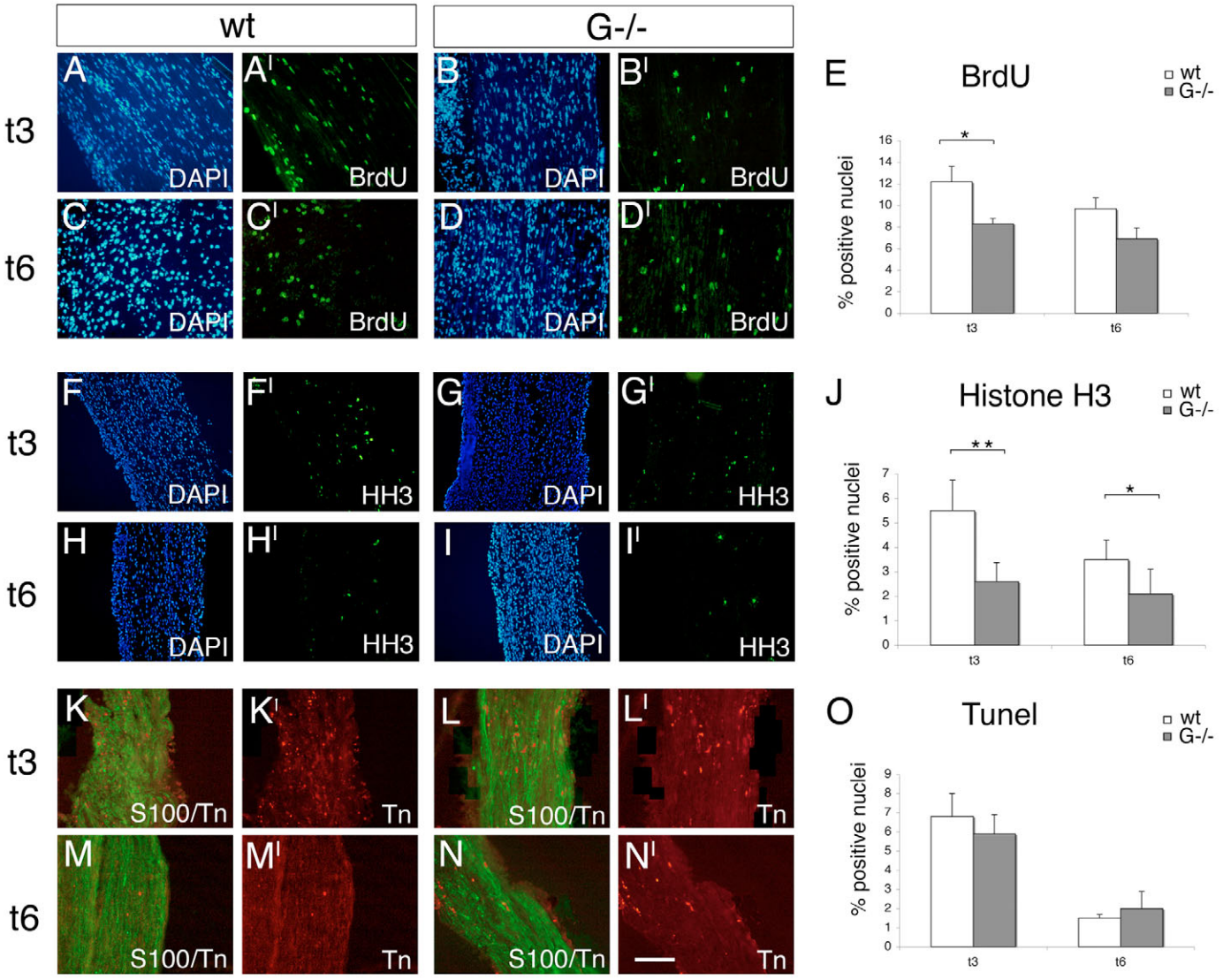

Fig. 6. Schwann cells in the distal stump of nerves of GFAP-null mice after injury show reduced proliferation but normal apoptosis. (A-D) Nuclei staining with DAPI (blue) and BrdU (green) on longitudinal sections of the distal stump of the sciatic nerve at 3 and 6 days (t3 and t6, respectively) after injury. The number of BrdU-positive nuclei is reduced at both t3 and t6 in nerves of mutant mice. (E) Quantitative analysis shows that the percentage of BrdU-positive nuclei is significantly decreased at t3 (*P=0.04) and consistently but not significantly reduced at t6 (P=0.06). (F-I) Staining of nuclei with DAPI (blue) and of phosphorylated histone H3 (green) on longitudinal sections of the distal stump of the sciatic nerve at days 3 and 6 after injury. The number of nuclei positive for phosphorylated histone H3 is reduced at both t3 and t6 in nerves GFAP-null mice. (J) Quantitative analysis shows that the percentage of phosphorylated histone H3 nuclei is significantly reduced at both t3 (**P<0.001) and t6 (*P=0.04). (K-N). S100 (green) and TUNEL (red) staining on longitudinal sections of the distal stump of the sciatic nerve at t3 and t6 after crushing. TUNEL staining shows a similar number of positive nuclei in mutant and control nerves at both time points. (O) Quantitative analysis shows no significant difference in the percentage of positive nuclei in mutants and controls. Error bars represent the ±s.e.m. Bar in N^I, 40 μm for A-D; 80 μm for F-I and K-N.

is induced and modulated by complex interactions of ECM receptors and ECM molecules. They include the ECM molecules normally expressed in the endoneurium and those molecules that infiltrate the nerve as the result of blood-nerve barrier disruption, such as fibrin. Disruption of this signaling pathway interferes with Schwann cell proliferation.

We investigated whether known adhesion complexes involved in Schwann cell proliferation can interact with GFAP or vimentin. Although Schwann cells express several ECM receptors during development and adult life (Milner et al., 1997; Previtali et al., 2003b), two adhesion pathways have been proposed to function after nerve injury. First, fibrin interacts with integrin αvβ8, which signals the occurred damage and stimulate Schwann cell proliferation (Akassoglou et al., 2003; Akassoglou et al., 2002; Chernousov and Carey, 2003). Then, the reorganization of the ECM allows fibronectin-integrin α5β1 interaction that carries on signaling for Schwann cell proliferation and differentiation to complete regeneration (Chernousov and Carey, 2003; Haack and Hynes, 2001; Lefcort et al., 1992). We therefore investigated whether GFAP and/or vimentin participate in the fibrin-αvβ8 and/or fibronectin-α5β1 complex. The homogenate of rat sciatic nerve was immunoprecipitated by using antisera against GFAP or vimentin. The immunoprecipitates were analyzed by western blotting using antibodies against integrin αv, α5, β1 and β8. Two different anti-GFAP antibodies (mouse and rat) but not anti-vimentin co-precipitated integrin subunits αv and β8 (Fig. 7A). By contrast, two different anti-vimentin antibodies (rabbit and mouse) but not anti-GFAP co-precipitated integrin subunits α5 and β1 (Fig. 7A). To confirm that vimentin cannot associate with αv integrin in the absence of GFAP, we performed further experiments with nerves of mutant and control mice. In the homogenate of nerves from GFAP-null mice, the anti-vimentin antibody did again not precipitate αv integrin, whereas αv integrin was immunoprecipitated by GFAP in nerve homogenates of control mice (Fig. 7B).

It has been reported that the fibrin–αvβ8-integrin pathway modulates Schwann cell proliferation by phosphorylating ERK1/2 [p44/42 MAP kinase (MAPK)] (Akassoglou et al., 2002). We first verified that ERK1/2 phosphorylation is the cause and not the consequence for reduced Schwann cell proliferation. The sciatic nerves of ten 3-months old mice were crushed. Five mice were treated with the MAP kinase kinase (MEK) inhibitor PD098059, which blocks ERK1/2 phosphorylation and compared to the other five mice treated

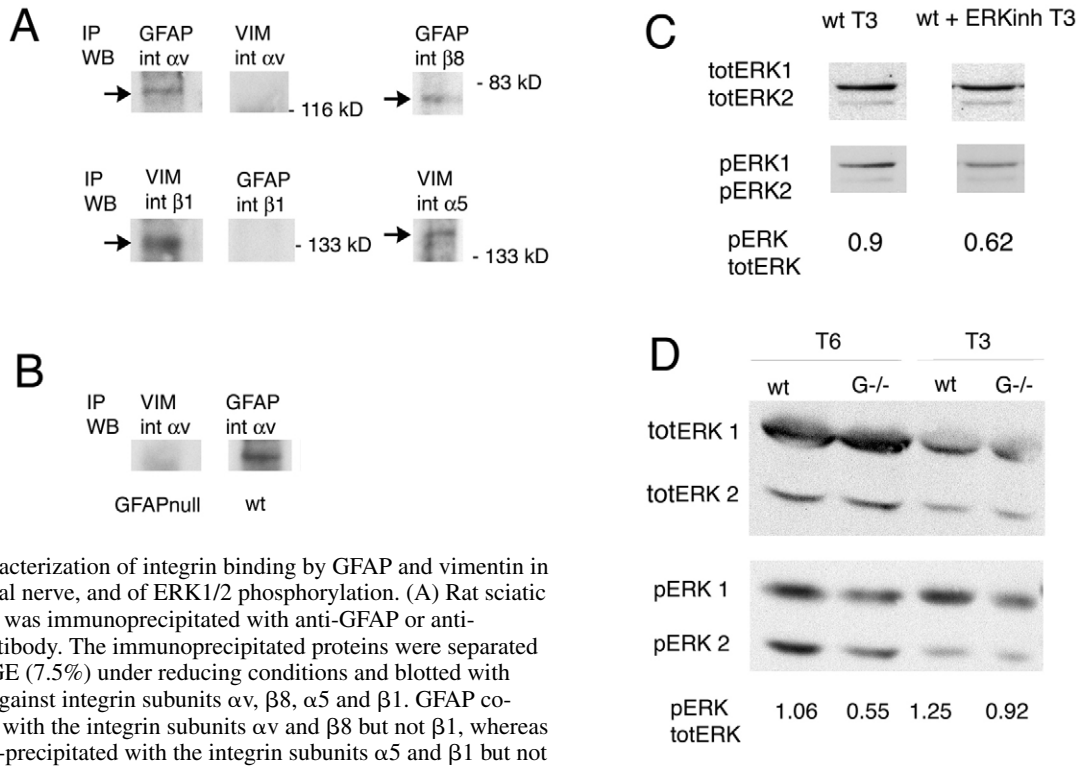

Fig. 7. Characterization of integrin binding by GFAP and vimentin in the peripheral nerve, and of ERK1/2 phosphorylation. (A) Rat sciatic nerve lysate was immunoprecipitated with anti-GFAP or anti-vimentin antibody. The immunoprecipitated proteins were separated in SDS-PAGE (7.5%) under reducing conditions and blotted with antibodies against integrin subunits αv, β8, α5 and β1. GFAP co-precipitated with the integrin subunits αv and β8 but not β1, whereas vimentin co-precipitated with the integrin subunits α5 and β1 but not αv. (B) Sciatic nerve lysate of GFAP-null mice was immunoprecipitated as described above with anti-vimentin antibody and blotted with anti-integrin αv antibody; similarly the wild-type sciatic nerve lysate was immunoprecipitated with anti-GFAP antibody and blotted with anti-integrin αv antibody. Vimentin still did not co-precipitate with integrin αv in GFAP-null mice lysate, whereas integrin αv again co-precipitated with GFAP in lysate of control-mice nerves. (C) Protein extracts form the distal stamp of wild-type mice treated with DMSO and wild-type mice treated with the MEK inhibitor PD098059 at 3 days (T3) after injury were immunoblotted with antibody against total ERK1/2 or phosphorylated ERK1/2. By densitometry the ratio of totalERK1/2 to pERK1/2 was measured and is stated below the blot as a number, indicates the phosphorylation state. Mice treated with PD098059 showed reduced ERK phosphorylation (D) Protein extracts from the distal stump of crushed nerves from wild-type and GFAP-null mice at T3 and T6 were immunoblotted with antibody against total ERK1/2 or phosphorylated ERK1/2. By densitometry, the ratio of totalERK1/2 to pERK1/2 was measured as described above. Nerves of GFAP-null mice showed less phosphorylated Erk1/2 compared with controls at both time points after injury.

with the vehicle (DMSO 10%). At 3 days post-injury, BrdU labeling of S100-positive cells showed Schwann cell proliferation reduced by 50% in mice treated with the PD098059 (9.5%±1.4 vs 4.5%±1.5, P=0.0003; data not shown). In the same animals, the homogenate of the crushed controlateral nerve confirmed reduced ERK1/2 phosphorylation by 25% (Fig. 7C)

Since we were able to show that GFAP is part of the fibrin–αvβ8-integrin pathway, we investigated whether defective Schwann cell proliferation in GFAP-null mice was associated with reduced ERK1/2 phosphorylation. The homogenates of the distal stump of T3 and T6 crushed nerve from GFAP-null and wild-type controls were compared by using an antibody specific for the phosphorylated form of ERK1/2. At both time points, the sciatic nerves of GFAP-null mice showed a reduction of ERK1/2 phosphorylation, by 27% at T3 and 48% at T6 compared with wild-type controls (Fig. 7D). The levels of total ERK1/2 were similar in GFAP-null mice and controls. Hence, the difference in ERK1/2 phosphorylation was not the consequence of different amounts of total ERK1/2.

Discussion

This study shows that GFAP modulates the Schwann cell response for tissue recovery after peripheral nerve injury. We provide evidence for the first time that, (1) GFAP is involved in Schwann cell proliferation, (2) GFAP is the cytoskeleton component of the previously identified pathway originated by fibrin that drives Schwann cell proliferation after damage, (3) GFAP and vimentin constitute two different pathways that link the Schwann cell cytoskeleton to the ECM, both of which involved in proliferation and differentiation. Finally, our study shows that GFAP is not necessary for the development of the peripheral nerve, probably compensated for by other intermediate filaments. Disruption or defective function of the GFAP pathway may therefore interfere with the regenerative capacity of the peripheral nerve that, in chronic conditions, might determine severe degenerative defects and axonal loss.

Vimentin and nestin probably compensate for the absence of GFAP during PNS development

It was shown previously by gene targeting inactivation that GFAP is not overtly required for normal mouse CNS development (Gomi et al., 1995; Liedtke et al., 1996; McCall et al., 1996; Pekny et al., 1995). Although these reports were focused on the CNS, we confirmed here that also the PNS develops normally. We investigated nerve development from birth to adulthood, and observed in GFAP-null mice normal timing of Schwann-cell–axon interactions, normal cyto-architecture of both myelin-forming and non-myelin-forming Schwann cells, and regular fiber-type distribution. Peripheral nerves also showed normal function in neurophysiological and functional tests. The lack of an evident phenotype might be the consequence of at least two events: (1) GFAP has no main role in Schwann cell development and nerve function and/or, (2) other molecules are redundant or can compensate for loss of GFAP.

Regarding the first point, GFAP appears at a relative late stage in Schwann cell development, basically when immature Schwann cells have formed already, and it is downregulated in those Schwann cells that form myelin (Jessen et al., 1990). In mature nerves, only non-myelin-forming Schwann cells and Schwann cells that dedifferentiate after nerve injury express GFAP (Jessen et al., 1990). Hence, most of the time developing Schwann cells do not express GFAP, whereas its expression is restricted to a short, temporary window. The role of GFAP, being mostly unknown and related to the cytoskeleton organization, may be therefore skipped and seems insignificant in the developing Schwann cells.

As to the second point, redundancy of and/or compensation by other intermediate filaments may mask GFAP deficiency in Schwann cell development. Schwann cells express two other intermediate filaments, nestin and vimentin, during their embryonic development, and vimentin is maintained at high levels also in mature Schwann cells (Dong et al., 1999; Jessen and Mirsky, 1991). We confirmed by qualitative and quantitative analyses that vimentin and nestin are expressed at similar amounts in mature GFAP-null Schwann cells compared with controls. Hence, redundancy might explain the absence of phenotype in the peripheral nerve of GFAP-null mice. Finally, mutant mice showed an increased amount of fibronectin in the endoneurium. Fibronectin is a potent promoter of peripheral neurite outgrowth both during development and regeneration (Lefcort et al., 1992). The increased expression of fibronectin might further favor nerve development in mutant mice independently by the presence of GFAP.

Loss of GFAP affects early Schwann cell proliferation thus causing delayed nerve regeneration

Although PNS function and development appeared normal in the absence of GFAP, nerve regeneration was delayed in GFAP mutants. In fact, the demand for intermediate filaments is highly increased in Schwann cell after damage. Both GFAP and vimentin are upregulated, perhaps to provide an efficient cytoskeleton rearrangement necessary for proliferation and differentiation (Gillen et al., 1995; Neuberger and Cornbrooks, 1989; Thomson et al., 1993). Thus, compensatory mechanisms might no longer be sufficient for the Schwann cell to support the loss of GFAP in an acute crisis, such as after injury. Accordingly, nerve regeneration in vivo and neurite outgrowth in vitro was described as being delayed in vimentin-null mice (Perlson et al., 2005). Whether delayed regeneration in vimentin-null mice depends exclusively on impaired retrograde transport of the perk–vimentin–dynein–importin-β complex in the damaged axons, or is the consequence of impaired function of vimentin-null Schwann cells, needs further investigation.

The observation that GFAP-null mice had a delay in nerve regeneration might be due to different scenarios: (1) defective Schwann cell dedifferentiation, (2) impaired proliferation, (3) defective organization into bands of Bungner or, (4) impaired interaction between Schwann cells and regrowing axons. The regular upregulation of vimentin and the coherent expression of markers of dedifferentiation, such as vimentin, L1, NCAM and $p75^{NTR}$, in GFAP-null Schwann cells after damage suggested a normal dedifferentiation process. Moreover, GFAP-null Schwann cells could organize Bungner bands, which appeared morphologically normal – although only with a delay. Finally, we observed – although not in detail – normal Schwann cell-axon interaction by morphological analysis and expression of L1/NCAM/NF markers.

Our results provided evidence that defective regeneration is probably the consequence of reduced Schwann cell

proliferation after damage. Soon after nerve injury, dedifferentiated Schwann cells enter the cell cycle to provide a sufficient substrate for nerve regrowth. Previous studies showed that Schwann cells highly proliferate in the first week post injury, with a peak at day 3 (Clemence et al., 1989; Oaklander and Spencer, 1988; Pellegrino et al., 1986). Our results of BrdU (labeling cells in G1-S-M phase) and histone H3 (labeling cells in M phase) analyses in nerves of control mice confirmed data previously reported on Schwann cell proliferation after injury, and showed a significant reduction in the number of mitotic Schwann cells in GFAP mutants. Reduced proliferation was statistically significant at days 3 and 6 for histone H3 and at day 3 for BrdU, and very close to significance at day 6 for BrdU (P=0.06). Apoptosis was not modified by the absence of GFAP, suggesting a defect in proliferation and not in cell survival. Accordingly we found a reduction in ERK1/2 phosphorylation in nerves of mutant mice. Activation of the MAP-kinase pathway regulates transcription of genes associated with proliferation and differentiation in several cell types (Cowley et al., 1994; Kotch, 2000), including Schwann cells (Akassoglou et al., 2002). As confirmed by our results with the ERK inhibitor, the MAP-kinase pathway is at least one of the pathways that regulate Schwann cell proliferation after injury. In fact, we found that Schwann cell proliferation and ERK1/2 phosphorylation was reduced but not abolished in nerves of mutant mice. Several receptors and molecular pathways sustain proliferation. We probably interfered with only one of these pathways, which requires fibrin deposition and integrin αvβ8 activation, and is specifically active in the first steps of nerve regeneration (Akassoglou et al., 2003; Akassoglou et al., 2002).

A potential role for GFAP in cell proliferation has also been suggested previously (Yasui et al., 1998; Kawajiri et al., 2003). Cytoskeleton reorganization and cytoplasm segregation is a crucial step in cell proliferation and division. In particular, several intermediate filaments are phosphorylated during mitosis and continuously shift from an assembled (filamentous) to a disassembled (soluble) state. Rho-kinases phosphorylate GFAP, thereby causing their disassembly to accomplish cytokinesis (Yasui et al., 1998). Similarly, Aurora-B kinase, required for chromosome segregation and mitosis, was recently reported to phosphorylate a number of intermediate filaments including GFAP (Kawajiri et al., 2003). Our findings suggest that the role of GFAP in proliferation is cell-specific or, more likely, specific to the cell environment and stimuli. Increased astrocyte proliferation and GFAP overexpression is also observed in reactive astrocytosis in CNS. However, when GFAP is deleted reactive astrocytosis is not impaired and BrdU-pulse investigation failed to demonstrate proliferative abnormalities in GFAP mutant astrocytes (Pekny et al., 1999).

GFAP and vimentin link ECM to the Schwann cell cytoskeleton via two distinct pathways

We found that GFAP and vimentin bind to integrin αvβ8 and integrin α5β1, respectively, two ECM-receptors involved in Schwann cell proliferation and nerve regeneration (Akassoglou et al., 2003; Akassoglou et al., 2002; Chernousov and Carey, 2003; Haack and Hynes, 2001; Lefcort et al., 1992). This was not a surprise. As transmembrane receptors, integrins physically interact, directly or through cytolinker molecules, with cytoskeleton constituents including intermediate filaments (Herrmann and Aebi, 2000; Kreis et al., 2005; Rutka et al., 1997). Intermediate filaments participating in these cross-bridges probably constitute a link between cell surface and nucleus (Maniotis et al., 1997). This interaction provides a structural framework to facilitate intracellular responses, including protein phosphorylation, intracellular pH and Ca^{2+} modification, and the activation of MAP kinase cascades (Turner, 2000). These signaling events culminate in the reorganization of the cytoskeleton necessary for motility, proliferation and gene expression.

Our results suggested that the interaction of intermediate filaments and integrins was specific and segregated. GFAP associated with integrin αvβ8 but not integrin α5β1, whereas vimentin associated with integrin α5β1 but not integrin αvβ8, thus also excluding non-specific binding. However, we do not know whether this is a direct interaction or whether it is mediated by docking molecules. In the absence of GFAP, vimentin still associates with integrin α5β1 and not with integrin αvβ8, therefore explaining why vimentin can not compensate for the absence of GFAP in transducing the fibrin–integrin-αvβ8 signaling that is initiated early after damage. The Fibrin–integrin-αvβ8–GFAP complex probably drives Schwann cell proliferation only in close relation to nerve damage, whereas other pathways modulate Schwann cell mitosis in other situations. For example, in embryogenesis integrin α5β1 and fibronectin control the proliferation of Schwann cell progenitors, which express vimentin and not GFAP (Haack and Hynes, 2001; Lefcort et al., 1992; Peters and Hynes, 1996). Similarly, in the advanced phase of nerve regeneration Schwann cell proliferation is controlled by fibronectin and integrin α5β1 (Akassoglou et al., 2003; Akassoglou et al., 2002). Our results would fit with these previous observations. After nerve damage, the immediate repair reaction is sustained by the temporary ECM matrix formed by blood-derived fibrin, which immediately activates Schwann cell proliferation via the integrin-αvβ8–GFAP pathway. The absence of GFAP in our mutants would therefore block this early signal for Schwann cell proliferation. Later on, a mature ECM-scar is formed by fibronectin, which substitutes fibrin to sustain Schwann cell proliferation and initiates tasks for differentiation. The presence of different pathways that regulate Schwann cell proliferation between regeneration and development is not surprising. For example, cyclin D1 regulates Schwann cell proliferation in nerve regeneration but not in development (Atanasoski et al., 2001; Kim et al., 2000).

Finally, although the MAP-kinase pathway that drives cell proliferation might be directly initiated by integrins (Aplin et al., 2001), this pathway is more likely the consequence of collaborative signaling, in which integrin-mediated events are initiated by other types of receptors, primarily tyrosine-kinase growth-factor receptors (Assoian and Schwartz, 2001; Howe et al., 1998). For example, ErbB receptors and TGF-β have been already associated with Schwann cell proliferation in vivo and in vitro, and in different steps of nerve development (reviewed in Mirsky and Jessen, 2005). It is tempting to speculate that an extracellular fibrin (or fibronectin) network helps to accumulate integrin receptors in a restricted area of the Schwann cell surface, whereas intracellularly the GFAP (or vimentin) cytoskeleton helps to cluster the tyrosine-kinase receptors to initiate the MAP-kinase signaling pathway.

Can defective GFAP explain impaired regeneration in peripheral neuropathy?

Overall, our data showed that GFAP-null mice have delayed nerve regrowth and functional recovery after injury. Impairment in nerve regrowth was more evident in the first 2 weeks after damage, probably due to a reduced capacity of Schwann cells to proliferate and therefore to organize the regenerative scar. However, morphological and functional differences were still present 45 days after injury, at a time when repair is almost complete in control mice. The mutant mice showed reduced numbers of regrowing axons at all times and at 45 days still 20% of fibers were missing. Moreover, the difference in regrowth was more significant for larger axons.

Our data sustain that nerve repair is partially impaired but not abolished in GFAP mutants, whereas nerve development and function is not affected. This raises the possibility that *GFAP* mutations may affect the peripheral nerve. From this point of view, we may envisage three scenarios. (1) *Gfap* mutations give rise to peripheral neuropathy. These are probably not loss-of-function but gain-of-function mutations, because GFAP-null mice did not show peripheral neuropathy. Gain-of-function mutations in human are responsible for a severe leukodystrophy, Alexander disease (Messing and Goldman, 2004). The severity of Alexander disease might mask a more modest peripheral neuropathy, in a way similar to what occurred with the neuropathy associated with congenital muscular dystrophy in mutations in the laminin α2 gene (*LAMA2*) (Shorer et al., 1995). (2) GFAP dysfunction is not the consequence of genomic mutation but due to post-translational defects, i.e. phosphorylation or glycosylation. Something similar has been described for defective dystroglycan glycosylation. Mutations in genes that encode proteins that glycosylate the α-dystroglycan cause congenital muscular dystrophies in human and/or neuropathy in mice (Levedakou et al., 2005; Muntoni et al., 2004). (3) *GFAP* mutations do not cause a peripheral neuropathy, but reduce the capacity of nerve repair in course of genetic or acquired neuropathies. In this case, the modest delay in regeneration we saw in GFAP-mutant mice after a single pathogenetic event, may become more relevant by adding the delay in regeneration of several fibers in the presence of a prolonged and/or continuous damage.

Materials and Methods

Generation of GFAP-null mice

Generation of GFAP-null mice and characterization of their CNS has been described before (McCall et al., 1996); mice have been subsequently made congenic on an inbred C57BL/6 background. Animals were generated from our colony and genotyped by PCR analysis of genomic DNA from tail clips. All experiments were performed following the institutional guidelines.

Sciatic nerve crush-lesion

Adult mice were anesthetized with avertin (trichloroethanol, 0.02 ml/g of body weight) and crush injury was performed as described (Quattrini et al., 1996). After skin incision, the sciatic nerve was exposed and crushed distal to the sciatic notch for 20 seconds with fine forceps previously cooled in dry ice. To identify the site of injury, forceps were previously dropped into vital carbon. The nerve was replaced under the muscle and the incision sutured.

Rotarod analysis

Five 3-month-old GFAP-null mice and five 3-month-old control littermates were placed on a round metal bar, first rotating at four rotations per minute and then accelerating at 7.2 rpm (Ugo Basile, Como, Italy). The animals were allowed to stay on the rod for a maximum of 700 seconds and the time they stayed on the rotating rod was measured in subsequent trials (four trials in the first 2 days and one trial on each of 3 consecutive days).

Neurophysiological analysis

Five 3-month-old GFAP-null mice and five 3-month-old control littermates were analyzed, as described (Bolino et al., 2004), before crush injury and 10, 15, 21 and 45 days after crush injury. Mice were anesthetized with avertin and placed under a heating lamp to avoid hypothermia. The sciatic nerve conduction velocity (NCV) was obtained by stimulating the nerve with steel monopolar needle electrodes. A pair of stimulating electrodes was inserted subcutaneously near the nerve at the ankle. A second pair of electrodes was placed at the sciatic notch, to obtain two distinct sites of stimulation, proximal and distal along the nerve. The muscular response to the electrical nerve stimulation, compound motor action potentials (cMAP), was recorded with a pair of needle electrodes; the active electrode was inserted in muscles in the middle of the paw, while the reference was placed in the skin between the first and second digit.

Antibodies and Immunohistochemistry

Antibodies used for immunohistochemistry and/or western blotting are listed in Table 1. Immunofluorescence on cryosections was performed as described (Previtali et al., 2003b), and examined with confocal (Biorad MRC 1024) or fluorescent microscope (Olympus BX).

Inhibitor of ERK1/2 phosphorylation

The MAP kinase kinase (MEK) inhibitor PD098059 (Sigma) was dissolved in dimethyl sulfoxide (DMSO) and stored in aliquots at –80° C. The compound was diluted in saline (NaCl) immediately before use to a final concentration of 1 mg/kg.

Table 1. List of the antibodies

Antigen	Species	Clone	Source
BrdU	Mouse	BMC9318	Roche
Collagen IV	Rabbit		Chemicon
β-Dystroglycan	Rabbit	AP83	K. Campbell
ERK1/2	Rabbit		Cell Signaling
pERK1/2	Mouse	E10	Cell Signaling
Fibronectin	Rabbit		Chemicon
GFAP	Mouse	GA5	Chemicon
GFAP	Rat	2.2B10	Zymed
pHistone H3	Rabbit	Ser10	Upstate
Integrin α1	Rabbit		Chemicon
Integrin α2	Rabbit		Chemicon
Integrin α3	Rabbit		Chemicon
Integrin α5	Rabbit		Chemicon
Integrin α6	Rat	GoH3	A. Sonnenberg
Integrin αv	Rabbit		Chemicon
Integrin β1	Rat	Mb1.2	Chemicon
Integrin β1	Rabbit		Chemicon
Integrin β1	Mouse	2B1	Chemicon
Integrin β4	Rabbit		Chemicon
Integrin β8	Goat	G17	Santa Cruz
L1	Rat	324	Chemicon
Laminin EHS	Rabbit		Sigma
Laminin α1	Rabbit	H300	Santa Cruz
Laminin α1	Rat	AL1	Chemicon
Laminin α2	Rat	4H8-2	Alexis
Laminin α4	Rabbit	H-194	Santa Cruz
Laminin α5	Mouse	4C7	Chemicon
Laminin β1	Rat	LT3	Chemicon
Laminin β2	Rabbit	1117+	R. Timpl
Laminin γ1	Rat	A5	Chemicon
Laminin γ3	Rabbit	H140	Santa Cruz
MAG	Mouse		Chemicon
NCAM	Rabbit		Chemicon
Nestin	Mouse	ab6142	abcam
Neurofilament-H	Rabbit		Chemicon
Neurofilament-M	Mouse	NN18	Chemicon
p75NTR	Rabbit		Chemicon
S100	Mouse	SH-b1	Sigma
S100	Rabbit		Chemicon
β-Tubulin	Mouse	Tub2.1	Sigma
Vimentin	Rabbit		Chemicon
Vimentin	Mouse	LN-6	Sigma
Vitronectin	Rabbit	H270	Santa Cruz

PD098059 (0.4 ml volume), or an equivalent volume of the vehicle (DMSO 10%), was injected i.p. 2 hours after nerve injury and every 12 hours until mice were killed after 3 days for BrdU and western blotting experiments.

Immunoprecipitation and immunoblotting

Proteins were isolated from snap-frozen sciatic nerves of adult mice as described (Previtali et al., 2003a; Previtali et al., 2000). For western blot nerves suspended in Tris-buffered SDS lysis buffer (95 mM NaCl, 25 mM Tris-HCl pH 7.4, 10 mM EDTA, 2% SDS, protease or phosphatase inhibitors), sonicated and boiled. For immunoprecipitation, nerves were suspended in Igepal (Sigma, Milano, Italy) lysis buffer plus protease inhibitors and sonicated. Immunoprecipitations were performed with anti-GFAP (mouse or rat) and anti-vimentin (rabbit or mouse) for 3 hours at 4°C. The immune complexes were collected by 90 minutes incubation with protein-A or -G agarose beads (Sigma). After washing, antigens were separated by heating in reducing SDS sample buffer, and analyzed by SDS-polyacrilamide (PAGE) gel (8.5%). For western blotting, equal amounts of homogenates (5 μg) were diluted in 8M urea / 0.05M DTT, separated in sample buffer on 5 or 7.5% SDS-PAGE gel and transferred to PVDF (Millipore, Roma, Italy) or nitrocellulose membrane (Biorad, Segrate, Italy). Blots were blocked in PBS (0.05% Tween-5% dry milk) and incubated with the appropriate primary + peroxidase-conjugated secondary antibody (Sigma) and visualized by ECL (Amersham, Cologno M., Italy). The intensity of the bands was quantified by densitometry and the ratio between each antibody and β-tubulin, or phosphorylated ERK1/2 on total ERK1/2, was determined.

Retrograde labeling of motor neurons

Five 3-months old GFAP-null mice and five age-matched controls were anesthetized, the gastrocnemius muscle exposed, and 5 μl of 1% cholera toxin subunit B (Alexa Fluor-488 conjugate, Invitrogen, Burlingame, CA) in distilled water were injected into three different sites of the muscle. Mice were sacrificed 48 hours later and the lumbar enlargement of the spinal cord was harvested and postfixed with 4% paraformaldehyde. The spinal cord was cut in 20-μm thick sections with a cryostat. The three sections with the higher number of labeled motor neurons were chosen using a 20× objective, and the average numbers of neurons were compared.

BrdU, phosphoryated histone H3 and TUNEL analysis

BrdU (Roche, Monza, Italy) incorporation was performed as described (Feltri et al., 2002). We injected i.p. with 100 μg BrdU per g body weight 4 and 2 hours before killing six mice (three GFAP-null mice and three wt mice) 3 days after injury and a further six mice (three GFAP-null mice and three wt mice) 6 days after injury. The sciatic nerve was then processed for immunohistochemistry. Longitudinal nerve cryosections were first incubated with anti-BrdU antibody and anti-S100 antibody, then with secondary antibody, and nuclei were labeled with DAPI (Vector Laboratories, San Giuliano Milanese, Italy). Only rod-shaped nuclei associated with nerves were counted and the fraction of BrdU-positive nuclei was determined. At least 900 nuclei were examined. For histone H3 staining a further 6+6 animals were analyzed. Staining was performed similarly as described for BrdU. For terminal transferase dUTP nick-end-labeling (TUNEL) assay, the sciatic nerves were dissected, fixed 1 hour in 4% paraformaldehyde, and cryopreserved for immunohistochemistry. Sections were treated with acetone, stained with anti-S100 antibody and then processed for TUNEL as described (Grinspan et al., 1996). Nuclei were identified by DAPI staining. For quantification, DAPI-positive nuclei associated with nerves were counted and the fraction of TUNEL-positive nuclei was determined.

Light- and electron-microscopy

Morphological studies of semi-thin and ultra-thin nerve sections were performed as described (Previtali et al., 2000), and examined using a light- (Olympus BX51) or electron microscope (Zeiss CEM 902).

Morphometry

Digitalized images of fiber cross sections from corresponding levels of the sciatic nerve were obtained with a digital camera (Leica DFC300F) using a 100× objective. At least three images from five different animals per genotype at each time point were acquired (120×10^3 μm^2 of sciatic nerve per animal) and were analyzed with the Leica QWin software (Leica Mycrosystem). The g-ratio was determined by dividing the mean diameter of an axon without myelin by the mean diameter of the same axon with myelin. About 150 randomly chosen fibers per animal were analyzed. Statistical analysis was performed using Statview 5.0 software (SAS, Cary, NC).

We thank K. Campbell, U. Mueller, A. Sonnenberg and R. Timpl for the generous gift of antibodies. We also are indebted to A. Bolino, L. Wrabetz, M. L. Feltri and S. Amadio for critical reading of the manuscript and suggestions, to A. Bolis and C. Panzeri for technical assistance, and ALEMBIC for the use of the confocal microscope. This work was supported by grants from Telethon Italy (SCP, grant number GGP030193) and Ricerca finalizzata (AQ, grant number RF2003/171).

References

Akassoglou, K., Yu, W. M., Akpinar, P. and Strickland, S. (2002). Fibrin inhibits peripheral nerve remyelination by regulating Schwann cell differentiation. *Neuron* **33**, 861-875.

Akassoglou, K., Akpinar, P., Murray, S. and Strickland, S. (2003). Fibrin is a regulator of Schwann cell migration after sciatic nerve injury in mice. *Neurosci. Lett.* **338**, 185-188.

Aplin, A. E., Stewart, S. A., Assoian, R. K. and Juliano, R. L. (2001). Integrin-mediated adhesion regulates ERK nuclear translocation and phosphorylation of Elk-1. *J. Cell Biol.* **153**, 273-282.

Assoian, R. K. and Schwartz, M. A. (2001). Coordinate signaling by integrins and receptor tyrosine kinale in the regulation of G1 phase cell-cycle progression. *Curr. Opin. Genet. Dev.* **11**, 48-53.

Atanasoski, S., Shumas, S., Dickson, C., Scherer, S. S. and Suter, U. (2001). Differential cyclin D1 requirements of proliferating schwann cells during development and after injury. *Mol. Cell. Neurosci.* **18**, 581-592.

Bolino, A., Bolis, A., Previtali, S. C., Dina, G., Bussini, S., Dati, G., Amadio, S., Del Carro, U., Mruk, D. D., Feltri, M. L. et al. (2004). Disruption of Mtmr2 produces CMT4B1-like neuropathy with myelin outfolding and impaired spermatogenesis. *J. Cell Biol.* **167**, 711-721.

Chen, Y. Y., McDonald, D., Cheng, C., Magnowski, B., Durand, J. and Zochodne, D. W. (2005). Axon and Schwann cell partnership during nerve regrowth. *J. Neuropathol. Exp. Neurol.* **64**, 613-622.

Chernousov, M. A. and Carey, D. J. (2003). alphaVbeta8 integrin is a Schwann cell receptor for fibrin. *Exp. Cell Res.* **291**, 514-524.

Clemence, A., Mirsky, R. and Jessen, K. R. (1989). Non-myelin-forming Schwann cells proliferate rapidly during Wallerian degeneration in the rat sciatic nerve. *J. Neurocytol.* **18**, 185-192.

Coulombe, P. A. and Wong, P. (2004). Cytoplasmic intermediate filaments revealed as dynamic and multipurpose scaffolds. *Nat. Cell Biol.* **6**, 699-706.

Cowley, S., Peternon, H., Kemp, P. and Marshall, C. J. (1994). Activation of MAP kinase kinase is necessary and sufficient for PC12 differentiation and for transformation of NIH 3T3 cells. *Cell* **77**, 841-852.

Dong, Z., Sinanan, A., Parkinson, D., Parmantier, E., Mirsky, R. and Jessen, K. (1999). Schwann cell development in embryonic mouse nerves. *J. Neurosci. Res.* **56**, 334-348.

Feltri, M., Graus-Porta, D., Previtali, S., Nodari, A., Migliavacca, B., Cassetti, A., Littlewood-Evans, A., Reichardt, L., Messing, A., Quattrini, A. et al. (2002). Conditional disruption of beta1 integrin in Schwann cells impedes interactions with axons. *J. Cell Biol.* **156**, 199-209.

Gillen, C., Gleichmann, M., Spreyer, P. and Muller, H. W. (1995). Differentially expressed genes after peripheral nerve injury. *J. Neurosci. Res.* **42**, 159-171.

Gomi, H., Yokoyama, T., Fujimoto, K., Ikeda, T., Katoh, A., Itoh, T. and Itohara, S. (1995). Mice devoid of the glial fibrillary acidic protein develop normally and are susceptible to scrapie prions. *Neuron* **14**, 29-41.

Griffin, J. W. and Hoffman, P. N. (1993). Degeneration and regeneration in the peripheral nervous system. In *Peripheral Neuropathy* (ed. P. Dyck, P. Thomas, J. Griffin, P. Low and J. Poduslo), pp. 361-376. Philadelphia: Saunders Co.

Grinspan, J. B., Marchionni, M. A., Reeves, M., Coulaloglou, M. and Scherer, S. S. (1996). Axonal interactions regulate Schwann cell apoptosis in developing peripheral nerve: neuregulin receptors and the role of neuregulins. *J. Neurosci.* **16**, 6107-6118.

Haack, H. and Hynes, R. (2001). Integrin receptors are required for cell survival and proliferation during development of the peripheral glial lineage. *Dev. Biol.* **233**, 38-55.

Herrmann, H. and Aebi, U. (2000). Intermediate filaments and their associates multi-talented structural elements specifying cytoarchitecture and cytodynamics. *Curr. Opin. Cell Biol.* **12**, 79-90.

Howe, A., Aplin, A. E., Alahari, S. K. and Juliano, R. L. (1998). Integrin signaling and cell growth control. *Curr. Opin. Cell Biol.* **10**, 220-231.

Jessen, K. R. and Mirsky, R. (1991). Schwann cell precursors and their development. *Glia* **4**, 185-194.

Jessen, K. R., Morgan, L., Stewart, H. J. and Mirsky, R. (1990). Three markers of adult non-myelin-forming Schwann cells, 217c(Ran-1), A5E3 and GFAP: development and regulation by neuron-Schwann cell interactions. *Development* **109**, 91-103.

Kawajiri, A., Yasui, Y., Goto, H., Tatsuka, M., Takahashi, M., Nagata, K. and Inagaki, M. (2003). Functional significance of the specific sites phosphorylated in desmin at cleavage furrow: Aurora-B may phosphorylate and regulate type III intermediate filaments during cytokinesis coordinatedly with Rho-kinase. *Mol. Biol. Cell* **14**, 1489-1500.

Kim, H. A., Pomeroy, S. L., Whoriskey, W., Pawlitzky, I., Benowitz, L. J., Sicinski, P., Stiles, C. D. and Roberts, T. M. (2000). A developmentally regulated switch directs regenerative growth of Schwann cells through cyclin D1. *Neuron* **26**, 405-416.

Kotch, W. (2000). Meaningful relationships: the regulation of the Ras/Raf/MEK/ERK pathway by protein interactions. *Biochem. J.* **351**, 289-305.

Kreis, S., Schonfeld, H.-J., Melchior, C., Steirer, B. and Kieffer, N. (2005). The intermediate filament protein vimentin binds specifically to a recombinant integrin α2/β1 cytoplasmic tail complex and co-localizes with native α2/β1 in endothelial cell focal adhesion. *Exp. Cell Res.* **305**, 110-121.

Lefcort, F., Venstrom, K., McDonald, J. A. and Reichardt, L. F. (1992). Regulation of the expression of fibronectin and its receptor, α5β1, during developing and regeneration of peripheral nerve. *Development* **116**, 767-782.

Levedakou, E. N., Chen, X.-J., Soliven, B. and Popko, B. (2005). Disruption of the mouse large gene in the enr and myd mutants results in nerve, muscle, and neuromuscular junction defects. *Mol. Cell. Neurosci.* **28**, 757-769.

Liedtke, W., Edelmann, W., Bieri, P. L., Chiu, F. C., Cowan, N. J., Kucherlapati, R. and Raine, C. S. (1996). GFAP is necessary for the integrity of CNS white matter architecture and long-term maintenance of myelination. *Neuron* **17**, 607-615.

Maniotis, A. J., Chen, C. S. and Ingber, D. E. (1997). Demonstration of mechanical connections between integrins, cytoskeletal filaments, and nucleoplasm that stabilize nuclear structure. *Proc. Natl. Acad. Sci. USA* **94**, 849-854.

Martini, R. (1994). Expression and functional roles of neural cell surface molecules and extracellular matrix components during development and regeneration of peripheral nerves. *J. Neurocytol.* **23**, 1-28.

McCall, M. A., Gregg, R. G., Behringer, R. R., Brenner, M., Delaney, C. L., Galbreath, E. J., Zhang, C. L., Pearce, R. A., Chiu, S. Y. and Messing, A. (1996). Targeted deletion in astrocyte intermediate filament (Gfap) alters neuronal physiology. *Proc. Natl. Acad. Sci. USA* **93**, 6361-6366.

Menet, V., Gimenez, Y., Ribotta, M., Chauvet, N., Drian, M. J., Lannoy, J., Colucci-Guyon, E. and Privat, A. (2001). Inactivation of the glial fibrillary acidic protein gene, but not that of vimentin, improves neuronal survival and neurite growth by modifying adhesion molecule expression. *J. Neurosci.* **21**, 6147-6158.

Messing, A. and Brenner, M. (2003). GFAP: functional implications gleaned from studies of genetically engineered mice. *Glia* **43**, 87-90.

Messing, A. and Goldman, J. E. (2004). Alexander disease. In *Myelin and its Diseases* (ed. R. A. Lazzarini), pp. 851-866. San Diego: Academic Press.

Milner, R., Wilby, M., Nishimura, S., Boylen, K., Edwards, G., Fawcett, J., Streuli, C., Pytela, R. and ffrench-Constant, C. (1997). Division of labor of Schwann cell integrins during migration on peripheral nerve extracellular matrix ligands. *Dev. Biol.* **185**, 215-228.

Mirsky, R. and Jessen, K. R. (2005). Molecular signaling in Schwann cell development. In *Peripheral Neuropathy*. Vol. 1 (ed. P. J. Dyck and P. K. Thomas), pp. 341-376. Philadelphia: Elsevier Saunders.

Muntoni, F., Brockington, M., Torelli, S. and Brown, S. C. (2004). Defective glycosylation in congenital muscular dystrophies. *Curr. Opin. Neurol.* **17**, 205-209.

Neuberger, T. J. and Cornbrooks, C. J. (1989). Transient modulation of Schwann cell antigens after peripheral nerve transection and subsequent regeneration. *J. Neurocytol.* **18**, 695-710.

Oaklander, A. L. and Spencer, P. S. (1988). Cold blockade of axonal transport activates premitotic activity of Schwann cells and wallerian degeneration. *J. Neurochem.* **50**, 490-496.

Patton, B., Miner, J., Chiu, A. and Sanes, J. (1997). Distribution and function of laminins in the neuromuscular system of developing, adult, and mutant mice. *J. Cell Biol.* **139**, 1507-1521.

Pekny, M., Leveen, P., Pekna, M., Eliasson, C., Berthold, C. H., Westermark, B. and Betsholtz, C. (1995). Mice lacking glial fibrillary acidic protein display astrocytes devoid of intermediate filaments but develop and reproduce normally. *EMBO J.* **14**, 1590-1598.

Pekny, M., Johansson, C. B., Eliasson, C., Stakeberg, J., Wallen, A., Perlmann, T., Lendahl, U., Betsholtz, C., Berthold, C. H. and Frisen, J. (1999). Abnormal reaction to central nervous system injury in mice lacking glial fibrillary acidic protein and vimentin. *J. Cell Biol.* **145**, 503-514.

Pellegrino, R. G., Politis, M. J., Ritchie, J. M. and Spencer, P. S. (1986). Events in degenerating cat peripheral nerve: induction of Schwann cell S phase and its relation to nerve fibre degeneration. *J. Neurocytol.* **15**, 17-28.

Perlson, E., Hanz, S., Ben-Yaakov, K., Segal-Ruder, Y., Seger, R. and Fainzilber, M. (2005). Vimentin-dependent spatial translocation of an activated MAP kinase in injured nerve. *Neuron* **45**, 715-726.

Peters, J. H. and Hynes, R. O. (1996). Fibronectin isoform distribution in the mouse. I. The alternatively spliced EIIIB, EIIIA, and V segments show widespread codistribution in the developing mouse embryo. *Cell Adhes. Commun.* **4**, 103-125.

Previtali, S. C., Quattrini, A., Fasolini, M., Panzeri, M. C., Villa, A., Filbin, M. T., Li, W., Chiu, S. Y., Messing, A., Wrabetz, L. et al. (2000). Epitope-tagged P(0) glycoprotein causes Charcot-Marie-Tooth-like neuropathy in transgenic mice. *J. Cell Biol.* **151**, 1035-1046.

Previtali, S., Feltri, M., Archelos, J., Quattrini, A., Wrabetz, L. and Hartung, H.-P. (2001). Role of integrins in the peripheral nervous system. *Prog. Neurobiol.* **64**, 35-49.

Previtali, S. C., Dina, G., Nodari, A., Fasolini, M., Wrabetz, L., Mayer, U., Feltri, M. L. and Quattrini, A. (2003a). Schwann cells synthesize alpha7beta1 integrin which is dispensable for peripheral nerve development and myelination. *Mol. Cell. Neurosci.* **23**, 210-218.

Previtali, S. C., Nodari, A., Taveggia, C., Pardini, C., Dina, G., Villa, A., Wrabetz, L., Quattrini, A. and Feltri, M. L. (2003b). Expression of laminin receptors in schwann cell differentiation: evidence for distinct roles. *J. Neurosci.* **23**, 5520-5530.

Privat, A. (2003). Astrocytes as support for axonal regeneration in the central nervous system of mammals. *Glia* **43**, 91-93.

Quattrini, A., Previtali, S., Feltri, M. L., Canal, N., Nemni, R. and Wrabetz, L. (1996). β4 integrin and other Schwann cell markers in axonal neuropathy. *Glia* **17**, 294-306.

Rutka, J. T., Murakami, M., Dirks, P. B., Hubbard, S. L., Becker, L. E., Fukuyama, K., Jung, S., Tsugu, A. and Matsuzawa, K. (1997). Role of glial filaments in cells and tumors of glial origin: a review. *J. Neurosurg.* **87**, 420-430.

Scherer, S. S. and Salzer, J. L. (2001). Axon-Schwann cell interactions during peripheral nerve degeneration and regeneration. In *Glial Cell Development* (ed. K. R. Jessen and W. D. Richardson), pp. 299-330. Oxford: Oxford University Press.

Shorer, Z., Philpot, J., Muntoni, F., Sewry, C. and Dubowitz, V. (1995). Demyelinating peripheral neuropathy in merosin-deficient congenital muscular dystrophy. *J. Child Neurol.* **10**, 472-475.

Stoll, G. and Muller, H. W. (1999). Nerve injury, axonal degeneration and neural regeneration: basic insights. *Brain Pathol.* **9**, 313-325.

Thomson, C. E., Griffiths, I. R., McCulloch, M. C., Kyriakides, E., Barrie, J. A. and Montague, P. (1993). In vitro studies of axonally-regulated Schwann cell genes during Wallerian degeneration. *J. Neurocytol.* **22**, 590-602.

Turner, C. (2000). Paxillin and focal adhesion signalling. *Nat. Cell Biol.* **2**, E231-E236.

Webster, H. D. (1993). Development of peripheral nerve fibers. In *Peripheral Neuropathy*. Vol. I (ed. P. Dyck, P. Thomas, J. Griffin, P. Low and J. Poduslo), pp. 243-266. Philadelphia: Saunders Co.

Yasui, Y., Amano, M., Nagata, K., Inagaki, N., Nakamura, H., Saya, H., Kaibuchi, K. and Inagaki, M. (1998). Roles of Rho-associated kinase in cytokinesis; mutations in Rho-associated kinase phosphorylation sites impair cytokinetic segregation of glial filaments. *J. Cell Biol.* **143**, 1249-1258.